Journal of Nanofluids
Vol. 12, pp. 1614–1620, 2023
(www.aspbs.com/jon)

ARTICLE

Micropolar Hydromagnetic Fluid Over a Vertical Surface in Darcian Regime: An Analytical Approach

Mayzul Alom Hussain and Sahin Ahmed*

Department of Mathematics, Rajiv Gandhi University, Rono Hills, Doimukh, 791112, Arunachal Pradesh, India

In the present paper, the researcher investigates the mutual impact of radiative heat and mass exchange on hydromagnetic micropolar fluid moving along an infinite vertical surface in a porous regime. The goal of the research is to investigate the impact of convective temperature and mass flow on hydromagnetic motion of micropolar fluid across a vertical plate ingrained in a porous regime. The conservation equations with appropriate boundary conditions are resolved analytically by assuming a convergent series solution and thus obtained the analytical solutions for velocity, angular velocity (microrotation), temperature and molar-concentration. The novelty of the current work is that it takes heat transfer into account while considering for the impacts of chemical reaction in a micropolar fluid flow of reactive diffusing species. The influence of different physical variables on temperature, molar-concentration, velocity and angular velocity of the fluid molecules have been presented graphically for dual solutions. It is seen that the micropolar parameter and porosity of the medium play a significant behaviour over the momentum and thermal boundary layers. This investigation may involve with various disciplines of chemical engineering, bio-mechanics and medical sciences. The outcomes of the present study have significant applications in MHD generators and geothermal resource extraction.

KEYWORDS: Hydromagnetic, Micropolar, Porosity, Microrotation, MHD.

1. INTRODUCTION

The study of the interaction of conducting fluids and electromagnetic events is known as MHD. Micropolar fluids are micro structured fluids. Eringen[1,2] proposed the micropolar fluid theory, which consists of two distinct effects such as micro-rotational and micro-inertia. These investigations were driven by the latent standing of micropolar fluids in industrial sectors. The spirit of the micropolar fluid flow theory is that it extends the conservative equations for viscous fluids to include additional complicated fluids such as particle suspensions, liquid crystals, animal blood, lubrication, and turbulent shear flows. Ariman et al.[3,4] looked into the theory of micro structured fluids. The motion of micropolar fluid moving along a semi-infinite surface and plotted the outcomes over the velocity, micro-rotation, shear, and couple stresses studied by Hazarika and Ahmed.[5] He also discovered that when the micro-inertia is not constant, self-similar solutions can be obtained. The laminar boundary layer flow of a thermomicropolar fluid across a non-isothermal vertical flat surface and graphically depicted the impact of material characteristics on velocity and microrotation fields (Hazarika and Ahmed[6]). Peddieson[7] looked the boundary layer flow of a micropolar fluid across a flat plate and discovered that the model can predict results that have some of the same features as turbulent wall shear layers. However, the authors Nazar et al., Nadeem et al., and Olanrewaju et al.[8–10] were analysed the motion of molecules in hydromagnetic micropolar fluid at stagnation point, and the outcomes have been plotted graphically over the fluid properties. Many research has been approved to explore the influence of the exchange of mass and heat in micropolar fluid of porous material with MHD using various flow geometry such as vertical plate, semi-infinite plate, oscillating plate, stretching sheet, rotating cone, and so on.[11–22] Raptis[23] investigated the behaviour of micropolar fluid flowing along a plane of uniform motion with application of radiation and the outcomes asserts that augmented radiation, declined the temperature. Papautsky et al.[24] used a numerical model based on micropolar fluid theory to explore fluid behaviour in a rectangular microchannel. Researchers have done comparable work to investigate the combined effects of MHD free/forced convection, mass and heat transfer, and thermal radiation on fluid flow through a porous material.[25,26]

Problems of mutual heat and mass transport with the rate of reactions are significant in several processes and have thus gotten a lot of devotion in recent times and have lots of applications in the area of ventilation,

*Author to whom correspondence should be addressed.
Emails: sahin.ahmed@rgu.ac.in
Received: 22 July 2022
Accepted: 31 January 2023

disappearance at the surface of a water body, energy exchange in a tower of wet cooling, and the motion in a cooler of desert. Many sectors have potential applications for this type of flow. In the electric power business, for example, one method of generating electricity is to extract electrical energy directly from a moving conducting fluid. Khalid et al.[27] have published exact solutions using the Laplace transform approach for the exchange of heat and mass of micropolar fluid moving along an oscillating surface. The impact of heat radiation on unsteady free convective flow over a moving vertical plate with mass transfer and chemical reaction investigated by Muthucumaraswamy et al.[28] The Laplace transform approach was used to solve the dimensionless governing equations. Bakr[29] recently published an article for exchange of mass moving along a vertical surface of uniform motion for a rotating micropolar fluid under the application of heat source/sink and a reaction rate. Ahmed et al.[30] deliberate the consequence of the order one homogeneous molar reaction on the process of a non-steady motion along an infinite vertical surface with a uniform exchange of heat and mass. Chamkha[31] deliberate the behaviour of hydromagnetic along a stretched vertical permeable surface with uniform motion under the action of source/sink and a reaction rate. In a constant porosity porous media, Ahmed et al.[32] investigated the impacts of a force of inertia of molecules and viscous resistive force at the wall on flow and exchange of heat-convection. The exchange of convective heat across a stretched surface surrounded in a non-Darcian material of pores under the action of a magnetic field has explored by Abo-Eldahab and El Gendy.[33] Some recent notable works has been done by Krishna et al.[35–53] in the related field which are noteworthy to be mentioned, which provides inspiration for the current study.

The current work is motivated by the above investigations and focuses on hydromagnetic motion of micropolar fluid across a plane surface entrenched in a porous material under the action of micropolar parameter, porosity and thermal radiation. The dual solutions of the current research are obtained using analytical method via MATLAB codes.

2. MATHEMATICAL FORMULATION

The two-dimensional motion of viscous incompressible fluid of micropolar behaviour for Darcian porous material under the action of magnetic drag force has been considered in this investigation and the physical depiction of the situation has been initiated by Figure 1. Initially, the fluid and the plane surface are at rest, and then at $t > 0$ the surface set in uniform motion with velocity u_0 where T_w and C_w are the surface temperature and concentration respectively. The ambient temperature and concentration are respectively T_∞ and C_∞. The x-axis has set in the direction of fluid motion over the surface, while the axis of y-perpendicular to the surface. A uniform magnetic field

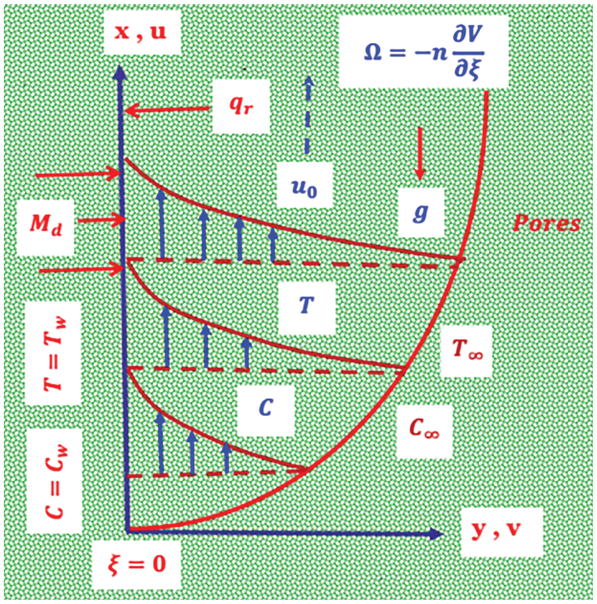

Fig. 1. Geometry of the flow configuration.

$(0, -B_o, 0)$ is acted to the fluid medium in a normal direction towards the surface.

The governing equations of the micropolar fluid over an oscillating vertical surface with thermophoretic forces are given as follows:[34]

$$\frac{\partial u}{\partial x} + \frac{\partial v}{\partial y} = 0 \Rightarrow \frac{\partial u}{\partial y} = 0 \tag{1}$$

$$\rho \frac{\partial u}{\partial t^*} = \begin{bmatrix} (\mu + \alpha)\frac{\partial^2 u}{\partial y^2} + \alpha \frac{\partial N}{\partial y} - \sigma {B_0}^2 u - \frac{\phi_1 \mu}{K} u \\ + \rho g \beta_T (T - T_\infty) + \rho g \beta_c (C - C_\infty) \end{bmatrix} \tag{2}$$

$$\rho j \frac{\partial N}{\partial t^*} = \upsilon \frac{\partial^2 N}{\partial y^2} \tag{3}$$

$$\rho C_p \frac{\partial T}{\partial t^*} = k_1 \frac{\partial^2 T}{\partial y^2} - \frac{\partial q_r}{\partial y} + \frac{D_m K_T}{C_s} \frac{\partial^2 C}{\partial y^2} \tag{4}$$

$$\frac{\partial C}{\partial t^*} = D_m \frac{\partial^2 C}{\partial y^2} - K_r (C - C_\infty) \tag{5}$$

The radiative heat influx is given by

$$\frac{\partial q_r}{\partial x} = -4a^2 (T - T_\infty) \tag{6}$$

The corresponding initial and boundary conditions are given by Ref. [34]

$$u = 0, \quad N = 0, \quad T = T_\infty, \quad C = C_\infty \quad \forall \ y \text{ at } t^* \le 0 \tag{7}$$

$$\left\{ \begin{array}{l} y = 0 : u = u_0, \quad N = -n\frac{\partial u}{\partial y}, \quad T = T_w, \quad C = C_w \\ y \to \infty : u \to 0, \quad N \to 0, \quad T \to T_\infty, \quad C \to C_\infty \end{array} \right\} \text{at } t^* > 0 \tag{8}$$

ARTICLE

Now, introducing the dimensionless variables,

$$\left\{\begin{array}{l} V=\dfrac{u}{u_0},\quad \xi=\dfrac{u_0}{\nu}y,\quad t=\dfrac{u_0^2}{\nu}t^*,\quad \Omega=\dfrac{\nu N}{u_0^2},\\ \theta=\dfrac{T-T_\infty}{T_w-T_\infty},\quad \phi=\dfrac{C-C_\infty}{C_w-C_\infty},\quad \beta=\dfrac{\alpha}{\mu},\\ M_d=\dfrac{\nu\sigma B_o^2}{\rho u_o^2},\quad G_r=\dfrac{\nu g\beta_T}{u_o^3\,(T_w-T_\infty)},\\ R_a=\dfrac{16\sigma_1 T_\infty^3}{3k_1k_2},\quad Gr_m=\dfrac{\nu g\beta_c}{u_o^3\,(C_w-C_\infty)},\\ K_P^{-1}=\dfrac{\nu^2\phi_1}{ku_o^2},\quad \eta=\dfrac{\mu j}{\gamma},\quad P_r=\dfrac{\mu C_p}{k_1},\quad Sc=\dfrac{\nu}{D}\\ K_{eff}=M_d+K^{-1},\quad Pr_{\text{eff}}=\dfrac{P_r}{(1+R_a)},\\ Du=\dfrac{D_mK_T\,(C_\omega-C_\infty)}{C_s\mu C_p\,(T_\omega-T_\infty)} \end{array}\right\} \tag{9}$$

With the help of these dimensionless variables (9), the Eqs. (2)–(5) are transformed as:

$$\frac{\partial V}{\partial t}=(1+\beta)\frac{\partial^2 V}{\partial\xi^2}+\beta\frac{\partial\Omega}{\partial\xi}-K_pV-M_dV+G_r\,\theta+Gr_m\,\phi \tag{10}$$

$$\frac{\partial\Omega}{\partial t}=\frac{1}{\eta}\frac{\partial^2\Omega}{\partial\xi^2} \tag{11}$$

$$\frac{\partial\theta}{\partial t}=\frac{1}{P_r}\frac{\partial^2\theta}{\partial\xi^2}+R_a\theta+Du\frac{\partial^2\phi}{\partial\xi^2} \tag{12}$$

$$\frac{\partial\phi}{\partial t}=\frac{1}{S_c}\frac{\partial^2\phi}{\partial\xi^2}-C_r\phi \tag{13}$$

The transformed initial and boundary conditions are:

$$V=0,\quad \Omega=0,\quad \theta=0,\quad \phi=0\quad \text{at}\quad t\le 0\ \ \forall\,\xi \tag{14}$$

$$t>0:\left\{\begin{array}{l} V=1,\quad \Omega=-n\dfrac{\partial V}{\partial\xi},\quad \theta=1,\\ \phi=1\quad \text{at}\quad \xi=0\\ v=0,\quad \Omega=0,\quad \theta=0,\\ \phi=0\quad \text{as}\quad \xi\to\infty \end{array}\right\} \tag{15}$$

3. SOLUTION OF THE GIVEN PROBLEM

By virtue of classical perturbation theory to solve the Eqs. (10)–(13), the convergent scheme of series solution is given by,

$$f(\xi,t)=f_0(\xi)+\epsilon\sum_{j=1}^{\infty}e^{i\omega t}f_j(\xi),\quad \epsilon\ll 1 \tag{16}$$

where $f\equiv v,\Omega,\theta$ or ϕ.

Table I. Analysis of M_d and R_a over the velocity (V) and temperature (θ) at $G_r=Gr_m=2$, $\beta=0.2$, $P_r=0.71$, $K_P=0.5$, $n=0.1$, $\eta=0.5$.

			Previous work[34]		Present work	
ξ	M_d	R_a	V	θ	V	θ
0.0	0.5	0.1	1.0	1.0	1.0	1.0
0.2	1.0	0.1	2.91038	0.41510	2.91210	0.41572
0.4	2.0	0.1	1.81034	0.10225	1.81052	0.10238
0.0	0.5	0.5	1.0	1.0	1.0	1.0
0.2	1.0	0.5	2.37058	0.50572	2.37107	0.50569
0.4	2.0	0.5	1.53071	0.10371	1.53067	0.10383

Applying Eq. (16) into Eqs. (10)–(13), we get the required solutions as

$$\phi=e^{-\sqrt{C_r\cdot\mathrm{Sc}}\,\xi} \tag{17}$$

$$\theta=Ae^{-\sqrt{R_a\cdot P_r}\,i\xi}+Be^{-\sqrt{C_r\cdot\mathrm{Sc}}\,\xi} \tag{18}$$

$$\Omega=n\left[\begin{array}{l}\sqrt{\dfrac{K_p+M_d}{1+\beta}}\left(1-\dfrac{G_r\cdot A}{C}+\dfrac{G_r\cdot B+Gr_m}{D}\right)\\ +i\cdot\sqrt{R_a\cdot P_r}\,\dfrac{G_r\cdot A}{C}-\sqrt{C_r\cdot\mathrm{Sc}}\cdot\dfrac{G_r\cdot B+Gr_m}{D}\end{array}\right]$$
$$+E\cdot\epsilon e^{i\omega t}e^{-\sqrt{i\omega\eta}\,\xi} \tag{19}$$

$$V=\left[\begin{array}{l}\left(1-\dfrac{G_r\cdot A}{C}+\dfrac{G_r\cdot B+Gm}{D}\right)e^{-\sqrt{\dfrac{K_p+M_d}{1+\beta}}\,\xi}\\ +\dfrac{G_r\cdot A}{C}e^{-\sqrt{R_a\cdot P_r}\,i\xi}\\ -\dfrac{G_r\cdot B+Gr_m}{D}e^{-\sqrt{C_r\cdot\mathrm{Sc}}\,\xi}\end{array}\right] \tag{20}$$

4. VALIDATION

The validation of the present investigation has been calculated with the previous work illustrated by Sheikh et al.[34] and they have not studied the impact of thermo-diffusion (D_u) and rate of reaction (C_r). The analysis of Table I recommend that the method of solution is stable and accurate which validates the considered flow model.

5. RESULTS AND DISCUSSION

The dual solutions for molar concentration, temperature, and velocity are obtained and the outcomes are plotted via MATLAB for various physical parameters, namely, Magnetic drag force (M_d), rate of Chemical reaction (C_r), Schmidt number (Sc), Dufour number (Du), porosity (K_P), Prandtl number (P_r), Mass Grashof number (Gr_m), Thermal Grashof number (G_r), Micropolar fluid parameter (β).

The physical parametric values of micropolar fluids have been chosen with regard to the physical point of view such as the application of higher porosity and lower porosity;

Higher magnetic field for strong action to the fluid; Higher and lower buoyancy forces; Maximum and endothermic reactions to the fluid; maximum and minimum angular rotations of the fluid. All the numerical calculations have been done via MATLAB code with respect to the default physical values otherwise stated and they are $R_a = \beta = 0.2$, $P_r = 0.71$, $G_r = Gr_m = 0.5$, $C_r = 0.1$, $M_d = 2$, $Du = 0.2$, $K_P = 0.01$, $n = 0.1$, $\eta = 0.5$, otherwise stated.

Figure 2 depicts the concentration profiles with ξ for various values of rate of chemical reaction (C_r) and Schmidt number (Sc). When C_r is positive, then the chemical reaction is endothermic. Due to the augmented values of endothermic chemical reaction, the molar concentration declined in the rotating fluid. The endothermic chemical reaction parameter always acts as a transfer of mass from source of the system to the environment of the considered surface. In the physical point of view, the Schmidt number may be expressed as $Sc =$ (kinematic viscosity)/(molecular diffusivity coefficient). The Schmidt number of species at 25 °C in Air ($Pr = 0.71$) have been considered as Ammonia ($Sc = 0.78$), Methanol ($Sc = 1.14$) and Ethanol ($Sc = 1.50$). The Schmidt numbers are $Sc = 1.14,\ 1.50 > 1$, and therefore the kinematic viscosity is dominant over the molecular diffusivity, while this behaviour is opposite in $Sc = 0.78$. The higher Schmidt number always thickened the molar concentration boundary layer.

Figure 3 portrays the temperature profiles with ξ for various values of endothermic chemical reaction ($C_r > 0$) and Dufour number (Du). In fluid mechanics, the number Du signifies the contribution of the concentration gradients to the thermal energy flux in the motion of flow. In Figure 3, the concentration gradients are dominant over the thermal energies in the motion of flow and therefore temperature depression has occurred due to the influence of the Dufour. The application of endothermic chemical reaction in the energy equation asserts that molecules of the reactive fluids did not generate kinematic energies and consequently there is a declination in temperature of the fluid. Also, it is perceived that higher rate of reaction near the surface possesses negative values due to higher rate of endothermic reaction.

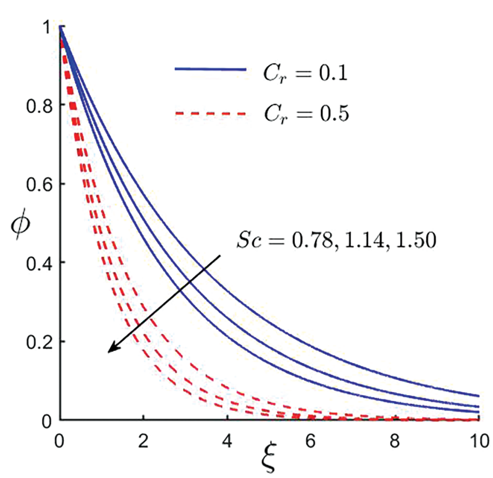

Fig. 2. Concentration profiles of Sc and C_r.

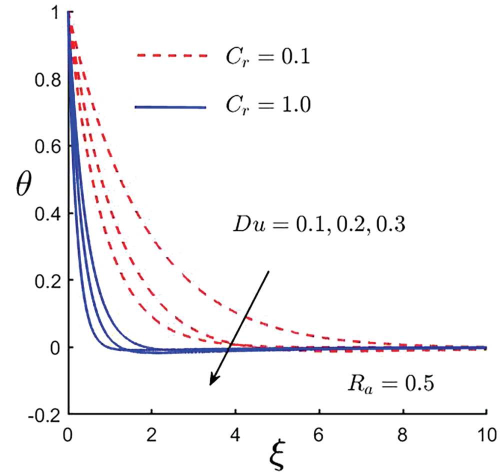

Fig. 3. Temperature profiles of C_r and Du.

The variation of porosity (K_P) and micropolar fluid parameter (β) have been calculated over the velocity distribution (V) and is plotted in Figure 4. The porosity of the porous material may performances as a resistive force that always retard the motion of the molecules of the fluid and thereby the momentum boundary layer thickness develops a thicker layer and gradually velocity deaccelerated throughout the motion. Moreover, the application of β decelerated the motion of molecules of micropolar fluid over the surface in porous regime. Under the simultaneous action of β and K_P the momentum boundary layer becomes thicker.

Figure 5 analysed the impact of Prandtl number (P_r) under the influence of molecular species of Ammonia ($Sc = 0.78$), and Ethanol ($Sc = 1.50$) in a Darcian regime. In physical point of view, P_r is encapsulated as $P_r =$ (kinematic viscosity (momentum diffusivity))/(thermal

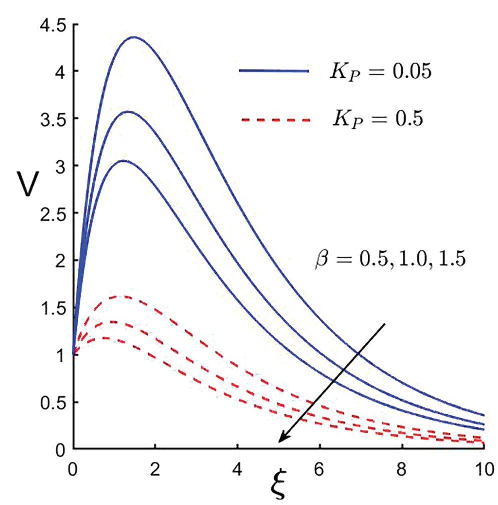

Fig. 4. Velocity profiles of K_P and β.

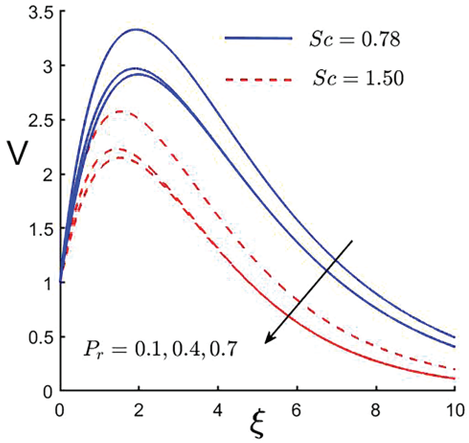

Fig. 5. Velocity profiles of P_r and Sc.

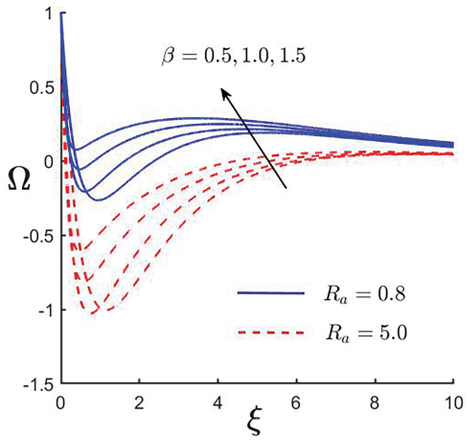

Fig. 7. Angular velocity profiles of β and R_a.

diffusivity) in a thermal boundary layer. As $P_r \leq 1$, so the kinematic viscosity is lower than the thermal diffusivity and thereby fluid molecules are diffused to get the higher values of momentum at $P_r = 0.1$. In porous media, fluid motion is inversely proportional to kinematic viscosity. Thus, in this Figure 5 it may observed that as P_r upsurges from lower value to higher values, there is a declination of fluid velocity due to the enhancement of kinematic viscosity. The Sc may be calculated as $Sc =$ (kinematic viscosity)/(molecular diffusivity). $Sc \geq 1$ implicates the kinematic viscosity is dominant over the molecular diffusivity coefficient. Higher Sc generates dominant kinematic viscosity and thereby lessening in fluid velocity, but lower $Sc < 1$ produces higher molecular diffusivity that gives resistance less motion of molecules uplifts the velocity. Therefore, the impact of Sc declines the motion of molecules from diffusivity to viscosity.

The dual solution of the velocity distribution for magnetic drag force (M_d) and buoyancy force (Gr_m) due to the exchange of mass has been presented in Figure 6. The

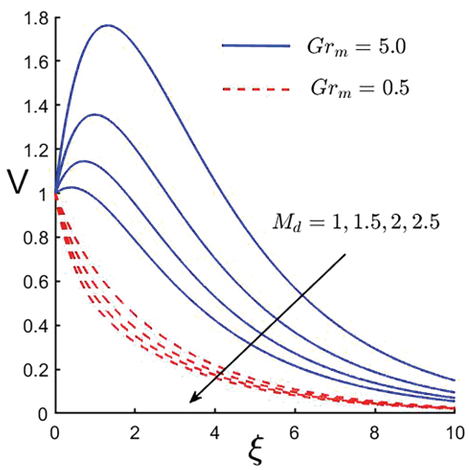

Fig. 6. Velocity profiles of M_d and Gr_m.

magnetic drag force has a retarding effect due to Lorentz force and thereby the molecules of the micropolar fluid are moving with slow motion. Hence, the flow velocity slowed by the impact of M_d and the momentum boundary layer thickness becomes thicker because the viscosity effect is pre-dominant near the surface. The buoyancy force is due to differences in pressure that boost the fluid velocity as the viscosity effect is very smaller and thereby molecules are moving freely in the upward direction opposite to acceleration due to gravity.

The impact of R_a and β have been discussed on the angular velocity (Ω) of the micropolar fluid and is shown in Figure 7. Higher thermal radiation ($R_a = 5.0$) produces lower thermal energy that causes the deceleration of angular velocity, while lower $R_a = 0.8$ generates the higher thermal energy that causes the acceleration in Ω. Therefore, the application of R_a declined the velocity Ω in the porous regime. The micropolar fluid parameter (β) boosted the curves of angular velocity in both the variant of R_a and all the curves of Ω are sustaining the asymptotic flow behaviour towards the free stream. Rotation of the micropolar fluid causes the high spin and generates vortex tubes that gets reversed motion towards the negative direction of the axis of rotation. The magnitude of micro-rotation show an increasing behaviour for higher values of R_a for different values of β.

The variation of angular velocity (Ω) by the influence of G_r and M_d has been illustrated in Figure 8. Physically, Grashof number indicates that $G_r =$ (buoyancy force)/(viscous force). The maximum spin of micropolar fluid in the formed vortex tube of angular velocity has been observed for the higher buoyancy force ($G_r = 15$), while slow rotation may occur at the lower buoyancy force ($G_r = 5$) and therefore a negative suppression has occurred in Ω along the vortex tube. The application of magnetic drag force (M_d) accelerates the angular velocity in the negative direction. The dual solutions of Ω encapsulated the motion of molecules asymptotically in the free

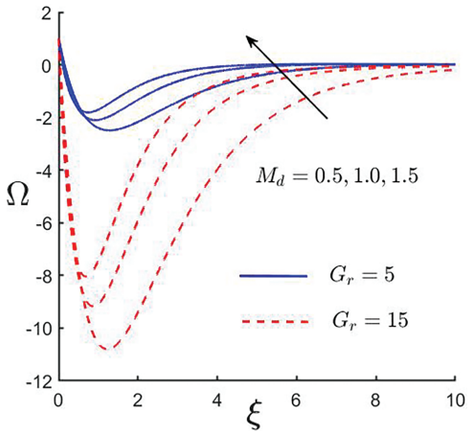

Fig. 8. Velocity profiles of G_r and M_d.

Table II. Distribution of Shear stress (τ_s) and couple stress (C_s) under the influence of M_d, Du, β and C_r at $G_r = Gr_m = 2$, $R_a = 0.2$, $P_r = 0.71$, $K_P = 0.1$, $n = 0.1$, $\eta = 0.5$.

β	M_d	Du	C_r	τ_s	C_s
0.01	0.5	0.1	0.1	8.13510	9.21073
0.05	0.5	0.1	0.1	7.62402	9.41970
0.5	0.5	0.1	0.1	7.40750	9.61891
0.01	**1.0**	0.1	0.1	8.50351	9.04165
0.01	**2.0**	0.1	0.1	8.7710	8.91532
0.01	0.5	**0.3**	0.1	10.7028	9.13051
0.01	0.5	**0.5**	0.1	32.10293	9.01752
0.01	0.5	0.1	**0.2**	8.47382	8.87105
0.01	0.5	0.1	**0.3**	8.61027	8.71962

stream. The magnitude of microrotation show a growing behaviour for greater values of G_r for different values of M_d.

The numerical values for the impact of M_d, Du, β and C_r over the τ_s and C_s are expressed in the Table II. The augmented values of M_d, Du and C_r enhanced the distributions of τ_s, while this behaviour is opposite to C_s. The shear stress has declined by the action of micropolar parameter, but this variable (β) up lift the profiles of couple stress in the Darcian regime.

6. CONCLUSION

In this investigation, a hydromagnetic micropolar fluid moving along a vertical surface entrenched in material of pores under the action of thermal radiation is considered. The dual solutions of the current work are obtained using analytical method. The important findings are concluded from the present work are that growth in Du and C_r, leads to declination in fluid temperature; upsurge in Sc and C_r, leads to falling of molar concentration in the rotating fluid; a rise in Sc and K_P, leads to declination of flow velocity in porous regime; an increase in M_d, β and P_r reduces the fluid velocity; rise in β and M_d, leads to declination of angular velocity, while this behaviour is opposite for the growth of G_r and R_a.

NOMENCLATURE

(x, y)	Cartesian coordinates, m
G_r	Thermal Grashof number
N	Dimensional angular velocity, S^{-1}
M_d	Magnetic drag force
P_r	Prandtl Number
R_a	Radiation parameter
Sc	Schmidt number
D_m	Mass diffusivity, m^2/s
K_{eff}, Pr_{eff}	Constants
B_0	Magnetic Induction, Tesla
g	Acceleration due to gravity, m/s^2
j	Microinertia per unit mass, $Kg \cdot m^2$
α	Vortex viscosity, ms^{-1}
μ	Dynamic viscosity, Pa s
β_T	Coefficient of thermal expansion, K^{-1}
σ	Electrical conductivity, Sm^{-1}
Du	Diffusion-thermo number
(u, v)	Velocity components in (x, y)-directions, ms^{-1}
Gr_m	Mass Grashof number
K_P	Porosity parameter
C	Species concentration, mol/m^3
C_p	Specific heat capacity, $J \cdot kg^{-1} \cdot K^{-1}$
C_s	Coefficient of couple stress, Pa
η	Spin gradient, s^{-1}
K_r	Chemical reaction coefficient, Ms^{-1}
k_T	Thermal diffusion ratio, m^2/s
K_P	Non-dimensional porosity, m^2
ω	Frequency parameter
ν	Kinematic viscosity, m^2s^{-1}
ρ	Fluid density, kgm^{-3}
k_1	Thermal conductivity, $W \cdot m^{-1}K^{-1}$
β_c	Coefficient of concentration expansion, K^{-1}
ϕ_1	Porosity of the porous medium $(0 < \phi_1 < 1)$, m^2
β	Micropolar fluid parameter

References and Notes

1. A. C. Eringen, *Int. J. Engng. Sci.* 2, 205 (**1964**).
2. A. C. Eringen, *J. Math. Mech.* 16, 1 (**1966**).
3. T. Ariman, M. A. Turk, and N. D. Sylvester, *Int. J. Engng. Sci.* 11, 905 (**1973**).
4. T. Ariman, M. A. Turk, and N. D. Sylvester, *Int. J. Engng. Sci.* 12, 273 (**1974**).
5. S. Hazarika and S. Ahmed, *Journal of Naval Architecture and Marine Engineering* 18, 25 (**2021**).
6. S. Hazarika and S. Ahmed, *J. Nanofluids* 9, 336 (**2020**).
7. J. Peddieson, *Int. J. Engng. Sci.* 10, 23 (**1972**).
8. R. Nazar, N. Amin, D. Filip, and I. Pop, *Int. J. Non-Linear Mechanics* 39, 1227 (**2004**).
9. S. Nadeem, M. Hussain, and M. Naz, *Meccanica* 45, 869 (**2010**).

ARTICLE

ARTICLE

10. P. O. Olanrewaju, G. T. Okedayo, and J. A. Gbadeyan, *Int. J. Applied Science and Technology* 1, 219 (**2011**).
11. S. R. Mishra, M. M. Hoque, B. Mohanty, and N. N. Anika, *Nonlinear Engineering-De Gruyter* 8, 65 (**2019**).
12. N. Shahid, *Springer Plus* 4, 1 (**2015**).
13. Y. J. Kim, *Transport in Porous Media* 56, 17 (**2004**).
14. S. Hazarika and S. Ahmed, *Walailak Journal of Science and Technology* 18, 1 (**2021**).
15. M. I. Haider, M. I. Asjad, R. Ali, F. Ghaemi, and A. Ahmadian, *J. Therm. Anal. Calorim.* 144, 2079 (**2021**).
16. S. Hazarika and S. Ahmed, *J. Nanofluids* 9, 336 (**2020**).
17. N. T. Eldabe, E. F. Elshehawey, E. M. E. Elbarbary, and N. S. Elgazery, *Applied Mathematics and Computation* 160, 437 (**2005**).
18. G. C. Hazarika, B. Phukan, and S. Ahmed, *J. Eng. Physics and Thermophysics (Springer)*, 93, 178 (**2020**).
19. D. Pal and S. Chatterjee, *Commun. Nonlinear Sci. Numer. Simulat.* 15, 1843 (**2010**).
20. K. Das, *Int. J. Heat and Mass Transfer* 54, 3505 (**2011**).
21. S. Ahmed, J. Zueco, and L. M. López-González, *Arabian Journal for Science and Engineering* 39, 5141 (**2017**).
22. S. Hazarika and S. Ahmed, *Mathematics and Computers in Simulation* 192, 452 (**2022**).
23. A. Raptis, *Int. J. Heat and Mass Transfer* 41, 2865 (**1998**).
24. I. Papautsky, J. Brazzle, T. Ameel, and A. B. Frazier, *Sensors and Actuators* 73, 101 (**1999**).
25. S. Ahmed, A. Batin, and A. J. Chamkha, *AEJ-Alexandria Engineering Journal* 54, 45 (**2015**).
26. S. Ahmed, J. Zueco, and L. M. López-Ochoa, *Chem. Eng. Commun.* 201, 419 (**2014**).
27. A. Khalid, I. K. A. Khan, and S. Shafie, *AIP Advances* 5, 1 (**2015**).
28. R. Muthucumaraswamy, P. Chandrakala, and S. A. Raj, *Int. J. Appl. Mech. Engrg*. 11, 639 (**2006**).
29. A. A. Bakr, *Commun. Nonlinear Sci. Numer. Simul*. 16, 698 (**2011**).
30. S. Ahmed, J. Zueco, and L. M. López-González, *Int. Journal of Heat and Mass Transfer* 104, 409 (**2017**).
31. A. J. Chamkha, *Int. Comm. Heat Mass Transfer* 30, 413 (**2003**).
32. S. Ahmed, J. Zueco, and L. M. López-González, *Int. Journal of Heat and Mass Transfer* 104, 409 (**2017**).
33. E. M. Abo-Eldahab and M. S. El Gendy, *Can. J. Phys*. 79, 1031 (**2001**).
34. N. A. Sheikh, F. Ali, I. Khan, M. Saqib, and A. Khan, *Mathematical Problems in Engineering* 2017, 1 (**2017**).
35. M. V. Krishna and A. J. Chamkha, *Results in Physics* 15, 102652 (**2019**).
36. M. V. Krishna, N. A. Ahammad, and A. J. Chamkha, *Case Studies in Thermal Engineering* 27, 101229 (**2021**).
37. M. V. Krishna, K. Bharathi, and A. J. Chamkha, *Interfacial Phenomena and Heat Transfer* 6, 253 (**2018**).
38. M. V. Krishna, K. Jyothi, and A. J. Chamkha, *Journal of Porous Media* 23, 751 (**2020**).
39. M. V. Krishna, P. V. S. Anand, and A. J. Chamkha, *Special Topics and Reviews in Porous Media: An International Journal* 10, 203 (**2019**).
40. M. V. Krishna, M. G. Reddy, and A. J. Chamkha, *International Journal of Fluid Mechanics Research* 46, 1 (**2019**).
41. M. V. Krishna and A. J. Chamkha, *International Communications in Heat and Mass Transfer* 113, 104494 (**2020**).
42. M. V. Krishna, M. G. Reddy, and A. J. Chamkha, *Journal of Porous Media* 24, 81 (**2021**).
43. M. V. Krishna and A. J. Chamkha, *International Journal of Ambient Energy* 43, 1 (**2021**).
44. M. V. Krishna, G. S. Reddy, and A. J. Chamkha, *Physics of Fluids* 30, 023106 (**2018**).
45. M. V. Krishna and A. J. Chamkha, *Physics of Fluids* 30, 053101 (**2018**).
46. A. Alagumalai, C. Qin, K. E. K. Vimal, E. Solomin, L. Yang, P. Zhang, T. Otanicar, A. Kasaeian, A. J. Chamkha, M. M. Rashidi, S. Wongwises, H. S. Ahn, Z. Lei, T. Saboori, and O. Mahian, *Nano Energy* 92, 106736 (**2022**).
47. T. Tayebi, A. S. Dogonchi, N. Karimi, H. Ge-JiLe, A. J. Chamkha, and Y. Elmasry, *Sustainable Energy Technologies and Assessments* 46, 101274 (**2021**).
48. A. J. Chamkha, A. S. Dogonchi, and D. D. Ganji, *Applied Sciences* 8, 2396 (**2018**).
49. S. M. Seyyedi, A. S. Dogonchi, M. Hashemi-Tilehnoee, D. D. Ganji, and A. J. Chamkha, *International Journal of Numerical Methods for Heat and Fluid Flow* 30, 4811 (**2020**).
50. A. S. Dogonchi, M. Waqas, S. R. Afshar, S. M. Seyyedi, M. Hashemi-Tilehnoee, A. J. Chamkha, and D. D. Ganji, *International Journal of Numerical Methods for Heat and Fluid Flow* 30, 659 (**2020**).
51. S. Eshaghi, F. Izadpanah, A. S. Dogonchi, A. J. Chamkha, M. B. B. Hamida, and H. Alhumade, *Case Studies in Thermal Engineering* 28, 101541 (**2021**).
52. A. S. Dogonchi, S. R. Mishra, A. J. Chamkha, M. Ghodrat, Y. Elmasry, and H. Alhumade, *Case Studies in Thermal Engineering* 27, 101298 (**2021**).
53. S. R. Afshar, S. R. Mishra, A. S. Dogonchi, N. Karimi, A. J. Chamkha, and H. Abulkhair, *Journal of the Taiwan Institute of Chemical Engineers* 128, 98 (**2021**).